

UC Berkeley

UC Berkeley Previously Published Works

Title

Least costly closed-loop performance diagnosis and plant re-identification

Permalink

<https://escholarship.org/uc/item/1cv5p3j9>

Journal

International Journal of Control, 88(11)

ISSN

0020-7179

Authors

Mesbah, A
Bombois, X
Forgione, M
[et al.](#)

Publication Date

2015-06-01

DOI

10.1080/00207179.2015.1040076

Peer reviewed

Least costly closed-loop performance diagnosis and plant re-identification

A. Mesbah^{a,*}, X. Bombois^b, M. Forgone^b, H. Hjalmarsson^c and P.M.J. Van den Hof^d

^aDepartment of Chemical and Biomolecular Engineering, University of California, Berkeley, CA, USA; ^bLaboratoire Ampère UMR CNRS, Ecole Centrale de Lyon, Ecully Cedex, France; ^cThe Automatic Control Laboratory, ACCESS Linnaeus Center, School of Electrical Engineering, KTH-Royal Institute of Technology, Stockholm, Sweden; ^dElectrical Engineering Department, Eindhoven University of Technology, Eindhoven, The Netherlands

(Received 26 September 2014; accepted 7 April 2015)

The inherent time-varying nature of dynamics in chemical processes often limits the lifetime performance of model-based control systems, as the plant and disturbance dynamics change over time. A critical step in the maintenance of model-based controllers is distinguishing control-relevant plant changes from variations in disturbance characteristics. In this paper, prediction error identification is used to evaluate a hypothesis test that detects if the performance drop arises from control-relevant plant changes. The decision rule is assessed by verifying whether an identified model of the true plant lies outside the set of all plant models that lead to adequate closed-loop performance. A unified experiment design framework is presented in the least costly context (i.e., least intrusion of nominal plant operation) to address the problem of input signal design for performance diagnosis and plant re-identification when the performance drop is due to plant changes. The application of the presented performance diagnosis approach to a (nonlinear) chemical reactor demonstrates the effectiveness of the approach in detecting the cause of an observed closed-loop performance drop based on the designed least costly diagnosis experiment.

Keywords: closed-loop performance diagnosis; hypothesis testing; prediction error identification; optimal experiment design

1. Introduction

In most industrial process control applications, the inherent (gradual) time-varying nature of the plant dynamics diminishes the lifetime performance of model-based control systems (see MacGregor & Cinar, 2012; Qin, 2012; Yin, Ding, Haghani, Hao, & Zhang, 2012; Shardt et al., 2012 for recent reviews on performance monitoring and diagnosis). Changes in the plant dynamics over time increase the plant-model mismatch, which may eventually invalidate the model identified at the commissioning stage of a model-based control system. In these circumstances, the common approach to restore the initial closed-loop performance level is to re-identify the plant dynamics in order to redesign the controller. However, re-identification of the plant dynamics often entails a high economic cost and, therefore, should be performed only when it is absolutely necessary (i.e., when the performance drop has been caused by a control-relevant plant change). In real practice, however, the closed-loop performance degradation mostly results from variations in disturbance characteristics or sensor and actuator failures. Hence, to avoid the excessive economic cost of the controller maintenance, a performance diagnosis step should be performed when a closed-loop performance drop is observed. The performance diagnosis should verify whether the performance degradation is due to a control-relevant plant change or due to variations in disturbance characteristics.

This paper presents a generic approach for the closed-loop performance diagnosis of model-based control systems. Figure 1 illustrates the notion of the proposed approach for performance diagnosis and plant re-identification. The performance of the closed-loop system is continuously monitored, e.g., by estimating the input/output variances and verifying whether the predetermined performance requirements are satisfied (see Huang & Shah, 1999). Once the performance monitoring algorithm detects a closed-loop performance drop, the performance diagnosis approach is launched to detect the cause of the degraded performance. As in most performance diagnosis approaches (Basseville, 1998; Benveniste, Basseville, & Moustakides, 1987; Gustafsson & Graebe, 1998), the diagnosis problem is formulated as a hypothesis test, which provides a statistical framework for making decisions between contradictory hypotheses (Kay, 1998). The to-be-distinguished hypotheses are (1) the performance drop is only due to variations in disturbance characteristics (hypothesis \mathcal{H}_0), and (2) the performance drop is due to a control-relevant plant change¹ (and possibly also due to variations in disturbance characteristics) (hypothesis \mathcal{H}_1). Note that when the hypothesis \mathcal{H}_0 holds, the plant can be different from that observed at commissioning, but the plant change does not lead to a performance drop. As shown in Figure 1, if the performance drop is due to variations in disturbance characteristics (\mathcal{H}_0 is the correct hypothesis),

*Corresponding author. Email: mesbah@berkeley.edu

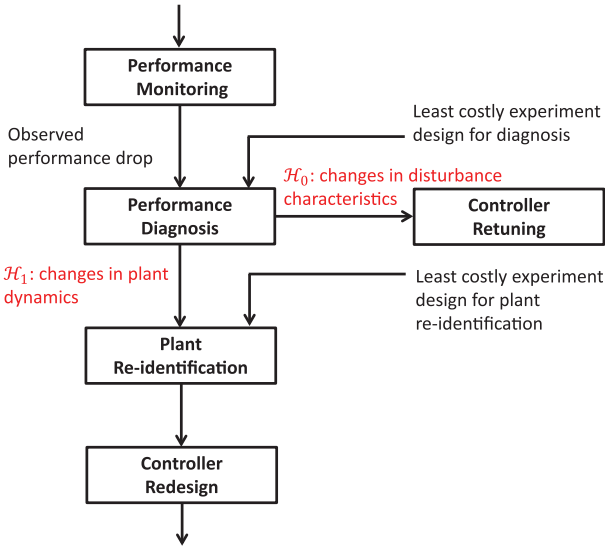


Figure 1. Procedure for performance diagnosis and plant re-identification.

the plant dynamics need not be re-identified and the closed-loop performance can be restored, e.g., by retuning the controller. On the other hand, if the performance drop is due to a control-relevant plant change (\mathcal{H}_1 is the correct hypothesis), the plant dynamics should be re-identified to redesign the controller.

The presented performance diagnosis approach does not depend on any a-priori assumptions on the possible plant and/or disturbance changes that may occur in the course of plant operation. This makes the performance diagnosis approach different from the set-based approaches (Olaru, De Doná, & Seron, 2008; Seron & De Doná, 2010), which can be used, for example, to detect sensor and actuator failures. In addition, as opposed to the more classical fault detection approaches (Basseville, 1998; Basseville & Benveniste, 1983; Benveniste et al., 1987; Huang & Tamayo, 2000; Jiang, Huang, & Shah, 2009), the diagnosis objective in this paper is not to detect any plant changes, but only those changes that lead to the closed-loop performance degradation (i.e., control-relevant changes). As in Gustafsson and Graebe (1998), Tyler and Morari (1996), the presented diagnosis approach is based on *cheap identification* of the true system with an economic cost much smaller than that when full re-identification should be performed for performance restoration. The advantage of using an identification approach as the basis for the diagnosis step is that the data collected for performance diagnosis can be readily used for the (eventual) full re-identification step, allowing for reducing the cost of the re-identification step. Like in Gustafsson and Graebe (1998), Tyler and Morari (1996), the presented approach relies on defining a set of all plant dynamics that result in a satisfactory closed-loop performance (with the existing controller under the original disturbance level) in order to examine the decision rule of the hypothesis test.

This paper also presents an optimal experiment design framework to design the diagnosis experiment in a least costly manner (see Bombois, Scorletti, Gevers, Van den Hof, & Hildebrand, 2006 for the notion of least costly identification). The experiment design problem is intended to minimize the cost of the diagnosis experiment, while guaranteeing a prespecified accuracy for the diagnosis. This allows for ensuring an optimal tradeoff between the contradictory objectives of obtaining an accurate diagnosis and of obtaining a *cheap* diagnosis experiment. To enable using the data collected during the diagnosis experiment for plant re-identification when \mathcal{H}_1 is the true hypothesis (see Figure 1), the experiment design framework also entails designing the possible re-identification experiment. The diagnosis and re-identification experiments are designed such that the re-identified model is accurate enough for redesigning the controller when \mathcal{H}_1 is selected in the decision rule. This implies that performance diagnosis and controller redesign can be unified in one framework, with the objective to reduce the overall cost of the maintenance of model-based controllers. Such a unified framework is an important step towards a cost-effective maintenance procedure for model-based controllers. This paper illustrates that the concept of least costly identification (Bombois et al., 2006) is a general paradigm that is not limited only to generating cheap and informative data for identification of an appropriate model for controller design, but can also be extended to performance diagnosis.

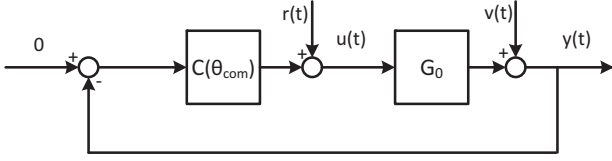
In this paper, the closed-loop performance diagnosis approach and the proposed decision rule are presented for linear time-invariant systems with disturbances described by a zero-mean stochastic process in the H_∞ -control setting² (Section 2). The post-performance diagnosis steps to restore the degraded closed-loop performance are thoroughly discussed. After formulating the unified optimal experiment design framework for performance diagnosis and possible plant re-identification (Section 3), a so-called two-scenario approach is presented to obtain initial model estimates that are required for solving the experiment design problem. The practical considerations pertaining to implementation of the proposed performance diagnosis approach are discussed (Section 4), and the effectiveness of the presented approach is demonstrated using a (nonlinear) CSTR case study (Section 5).

2. Closed-loop performance diagnosis

2.1 Hypothesis testing framework

Consider a stable linear time-invariant (LTI) single-input single-output system described by

$$y(t) = \underbrace{G(z, \theta_0)}_{G_0} u(t) + \underbrace{H(z, \theta_0)}_{v(t)} e(t), \quad (1)$$

Figure 2. Closed-loop system $[C(\theta_{\text{com}}) G_0]$.

where $y(t) \in \mathbf{R}$ is the system output, $u(t) \in \mathbf{R}$ is the system input, $\theta_0 \in \mathbf{R}^k$ is the unknown true parameter vector, $e(t)$ is a white noise signal with a covariance matrix σ_e^2 , $G(z, \theta_0)$ and $H(z, \theta_0)$ are stable discrete-time transfer functions. $H(z, \theta_0)$ is assumed to be monic and minimum-phase (Ljung, 1999). z denotes the shift operator.

Consider the closed-loop system in Figure 2 made up of the true system (1) and the controller $C(\theta_{\text{com}})$, which is designed based on a model $\{G(z, \theta_{\text{com}}), H(z, \theta_{\text{com}}), \hat{\sigma}_{e, \text{com}}^2\}$ of the true system (1) identified at the commissioning stage of the controller. In Figure 2, the excitation signal $r(t)$ is set to zero. At commissioning, the controller $C(\theta_{\text{com}})$ is designed to adequately reject the disturbance $v(t)$ (i.e., variances of the input and output signals should be reasonably small).

The H_∞ -control framework (e.g., see Zames, 1981; Zhou & Doyle, 1998) is used to measure the ability of the closed-loop system in rejecting the disturbances $v(t) = H_0(z)e(t)$ at commissioning. For a stable closed-loop system $[CG]$, made up of a plant G and a controller C , the performance measure is defined as

$$J(G, C, W_l, W_r) = \sup_{\omega} \bar{J}(\omega, G, C, W_l, W_r) \quad (2)$$

with

$$\begin{aligned} \bar{J}(\omega, G, C, W_l, W_r) &= \bar{\sigma} \left(W_l(e^{j\omega}) F(G(e^{j\omega}), C(e^{j\omega})) W_r(e^{j\omega}) \right) \\ F(G, C) &\triangleq \begin{pmatrix} \frac{GC}{1+GC} & \frac{G}{1+GC} \\ \frac{C}{1+GC} & \frac{1}{1+GC} \end{pmatrix}, \end{aligned} \quad (3)$$

where $\bar{\sigma}(A)$ denotes the largest singular value of A . W_l and W_r are some prespecified diagonal performance weight filters. The weight filters can be selected such that the performance measure is stated as a weighted function of $\frac{C}{1+GC}$ and $\frac{1}{1+GC}$. This enables relating the disturbance $v(t)$ to the plant inputs and outputs, respectively. The weights are chosen such that the loop $[C(\theta_{\text{com}}) G_0]$ (which satisfies $J(G_0, C(\theta_{\text{com}}), W_l, W_r) \leq 1$) rejects satisfactorily the disturbance $v(t)$ at commissioning. Next, the sets $\mathcal{D}_{\text{adm}}(C(\theta_{\text{com}}))$ and $\mathcal{V}_J(C(\theta_{\text{com}}))$ are defined to formulate the closed-loop performance diagnosis approach.

Definition 1: Consider the existing controller $C(\theta_{\text{com}})$ in the closed-loop system of Figure 2. $\mathcal{D}_{\text{adm}}(C(\theta_{\text{com}}))$ is defined as the set of all plant models G that are stabilised

by $C(\theta_{\text{com}})$ and lead to the nominal performance level $J(G, C(\theta_{\text{com}}), W_l, W_r) \leq 1$.

Definition 2: The set $\mathcal{V}_J(C(\theta_{\text{com}}))$ contains power spectra Φ_v of all disturbances $v(t)$ that are sufficiently rejected by all loops $[C(\theta_{\text{com}}) G]$ satisfying $J(G, C(\theta_{\text{com}}), W_l, W_r) \leq 1$. Disturbance $v(t)$ with spectrum Φ_v is considered to be sufficiently rejected by a loop $[CG]$ if the plant input and output signals have a reasonably small variance.

Definitions 1 and 2 suggest that the closed-loop performance of a loop $[C(\theta_{\text{com}}) G]$ is satisfactory only when $G \in \mathcal{D}_{\text{adm}}(C(\theta_{\text{com}}))$ and $\Phi_v \in \mathcal{V}_J(C(\theta_{\text{com}}))$. At commissioning, the controller $C(\theta_{\text{com}})$ is designed such that $G_0 \in \mathcal{D}_{\text{adm}}(C(\theta_{\text{com}}))$ and $\Phi_v \in \mathcal{V}_J(C(\theta_{\text{com}}))$. However, the plant dynamics G_0 or the disturbance spectrum Φ_v or most likely both plant dynamics and disturbance spectrum may change over time, possibly leading to the closed-loop performance deterioration. In the event of an observed performance drop (increased input/output variances), one of the following scenarios holds.

- (1) Even though G_0 might have changed, it remains in $\mathcal{D}_{\text{adm}}(C(\theta_{\text{com}}))$ while the disturbance spectrum no longer lies in $\mathcal{V}_J(C(\theta_{\text{com}}))$. This implies that the performance drop is due to the changes in disturbance characteristics.
- (2) G_0 has moved outside $\mathcal{D}_{\text{adm}}(C(\theta_{\text{com}}))$, suggesting that the changes in the plant dynamics G_0 have contributed to the performance drop (irrespective of the changes in the disturbance spectrum Φ_v).

Hence, using the performance set \mathcal{D}_{adm} , the hypothesis test pertaining to the closed-loop performance diagnosis problem can be formulated as

$$\begin{aligned} \mathcal{H}_0 &: G_0 \in \mathcal{D}_{\text{adm}}(C(\theta_{\text{com}})) \\ \mathcal{H}_1 &: G_0 \notin \mathcal{D}_{\text{adm}}(C(\theta_{\text{com}})). \end{aligned} \quad (4)$$

Equation (4) indicates that the observed performance drop is due to changes in disturbance spectrum when hypothesis \mathcal{H}_0 is true, and due to control-relevant plant changes (and possibly changes in disturbance characteristics) when \mathcal{H}_1 is true.

Remark 1: When \mathcal{H}_0 is the correct hypothesis, G_0 may not be the same as the plant dynamics at commissioning. The hypothesis test (4) indicates that the changes in G_0 (if there are any) do not lead to a performance drop. When \mathcal{H}_1 is the correct hypothesis, the disturbance spectrum may have also moved outside $\mathcal{V}_J(C(\theta_{\text{com}}))$. In this case, another hypothesis test can be performed in a similar manner as above to distinguish between $\Phi_v \in \mathcal{V}_J(C(\theta_{\text{com}}))$ and $\Phi_v \notin \mathcal{V}_J(C(\theta_{\text{com}}))$.

2.2 Decision rule

To discriminate between the two hypotheses stated in (4), the unknown true plant G_0 is identified in the closed-loop

$$P_{\hat{\theta}_N^{\text{det}}}^{-1} = N \underbrace{\left(\frac{1}{\sigma_e^2} \frac{1}{2\pi} \int_{-\pi}^{\pi} F_r(e^{j\omega}, \theta_0) F_r(e^{j\omega}, \theta_0)^* \Phi_{r,\text{det}}(\omega) d\omega \right)}_{\triangleq \mathcal{I}(\theta_0, \Phi_{r,\text{det}})} + N \left(\frac{1}{2\pi} \int_{-\pi}^{\pi} F_e(e^{j\omega}, \theta_0) F_e(e^{j\omega}, \theta_0)^* d\omega \right), \quad (10)$$

operation with the existing controller $C(\theta_{\text{com}})$. The signal $r(t) = r_{\text{det}}(t)$ (which is zero during the routine operation) is used to excite the closed-loop system for $(t = 0, \dots, N - 1)$ in order to collect the data $\{u(t), y(t) | t = 0, \dots, N - 1\}_{\text{det}}$ (see Figure 2). It is assumed that a full-order model parametrisation $\{G(z, \theta), H(z, \theta)\}$ can be constructed such that θ_0 in (1) is the only value of the parameter vector for which $\{G(z, \theta), H(z, \theta)\}$ represents the true plant. The parameter vector in this model structure is then identified based on $\{u(t), y(t) | t = 0, \dots, N - 1\}_{\text{det}}$ using the following criterion (Ljung, 1999)

$$\hat{\theta}_N^{\text{det}} = \arg \min_{\theta} V(\theta) \quad (5)$$

with

$$V(\theta) = \frac{1}{N} \sum_{t=0}^{N-1} \epsilon^2(t, \theta), \quad (6)$$

where $\hat{\theta}_N^{\text{det}}$ denotes the parameter vector obtained using the set $\{u(t), y(t)\}_{\text{det}}$ collected for performance diagnosis. The residuals $\epsilon(t, \theta) = H(z, \theta)^{-1}(y(t) - G(z, \theta)u(t))$ in (6) are related to $r(t) = r_{\text{det}}(t)$ via the measured signals $\{u(t), y(t)\}_{\text{det}}$

$$y(t) = S_0 v(t) + \underbrace{G_0 S_0 r(t)}_{y_r(t)} \quad (7)$$

$$u(t) = -C S_0 v(t) + \underbrace{S_0 r(t)}_{u_r(t)}, \quad (8)$$

where S_0 is the sensitivity function of the closed-loop system. This procedure gives a model $\hat{G}_N^{\text{det}} = G(z, \hat{\theta}_N^{\text{det}})$ of G_0 , along with a model $\hat{H}_N^{\text{det}} = H(z, \hat{\theta}_N^{\text{det}})$ of H_0 (with an estimate $\hat{\sigma}_e^2 = \frac{1}{N} \sum_{t=0}^{N-1} \epsilon^2(t, \hat{\theta}_N^{\text{det}})$ of σ_e^2).

The parameter vector $\hat{\theta}_N^{\text{det}}$ identified through (5) is asymptotically normally distributed around the true parameter vector θ_0 . Hence, $\hat{\theta}_N^{\text{det}} \sim \mathcal{N}(\theta_0, P_{\hat{\theta}_N^{\text{det}}})$, where $P_{\hat{\theta}_N^{\text{det}}}$ is a strictly positive definite matrix (Ljung, 1999)

$$\begin{aligned} P_{\hat{\theta}_N^{\text{det}}} &= \frac{\sigma_e^2}{N} \left(\bar{E} \left(\psi(t, \theta_0) \psi(t, \theta_0)^T \right) \right)^{-1} \text{ with } \psi(t, \theta) \\ &= -\frac{\partial \epsilon(t, \theta)}{\partial \theta}, \end{aligned} \quad (9)$$

where \bar{E} denotes the expected value. The covariance matrix can be estimated using $\hat{\theta}_N^{\text{det}}$ and $\{u(t), y(t)\}_{\text{det}}$. The inverse of the covariance matrix ($P_{\hat{\theta}_N^{\text{det}}}^{-1}$) can be expressed as

where $F_r(z, \theta_0) = S_0 \frac{\Lambda_G(z, \theta_0)}{H(z, \theta_0)}$, $F_e(z, \theta_0) = \frac{\Lambda_H(z, \theta_0)}{H(z, \theta_0)} - C(\theta_{\text{com}}) S_0 \Lambda_G(z, \theta_0)$, $\Lambda_G(z, \theta) = \frac{\partial G(z, \theta)}{\partial \theta}$, and $\Lambda_H(z, \theta) = \frac{\partial H(z, \theta)}{\partial \theta}$. Equation (10) implies that $P_{\hat{\theta}_N^{\text{det}}}^{-1} = \mathcal{I}(\theta_0, \Phi_{r,\text{det}})$ depends on the true plant (1) and is an affine function of the spectrum $\Phi_{r,\text{det}}$ of $r_{\text{det}}(t)$. The latter property will enable us to determine an optimal spectrum $\Phi_{r,\text{det}}$ for the diagnosis experiment.

Once a model \hat{G}_N^{det} of the true plant is obtained, it can be used to choose between hypotheses \mathcal{H}_0 and \mathcal{H}_1 (see (4)). The following decision rule is proposed to perform the hypothesis test

$$\begin{aligned} \hat{G}_N^{\text{det}} \in \mathcal{D}_{\text{adm}}(C(\theta_{\text{com}})) &\Rightarrow \text{choose } \mathcal{H}_0 \\ \hat{G}_N^{\text{det}} \notin \mathcal{D}_{\text{adm}}(C(\theta_{\text{com}})) &\Rightarrow \text{choose } \mathcal{H}_1. \end{aligned} \quad (11)$$

Equation (11) indicates that \mathcal{H}_0 is chosen as the correct hypothesis when \hat{G}_N^{det} is inside $\mathcal{D}_{\text{adm}}(C(\theta_{\text{com}}))$, whereas \mathcal{H}_1 is the correct hypothesis if \hat{G}_N^{det} lies outside $\mathcal{D}_{\text{adm}}(C(\theta_{\text{com}}))$. Verifying that $\hat{G}_N^{\text{det}} \in \mathcal{D}_{\text{adm}}(C(\theta_{\text{com}}))$ and $\hat{G}_N^{\text{det}} \notin \mathcal{D}_{\text{adm}}(C(\theta_{\text{com}}))$ can be straightforwardly done by evaluating if $J(\hat{G}_N^{\text{det}}, C(\theta_{\text{com}}), W_l, W_r) \leq 1$ and $J(\hat{G}_N^{\text{det}}, C(\theta_{\text{com}}), W_l, W_r) > 1$, respectively.

The decision rule (11) may lead to erroneous decisions since \hat{G}_N^{det} is an estimate of the true plant G_0 . Figure 3 illustrates the possibilities of making an erroneous decision. The null hypothesis \mathcal{H}_0 may be chosen erroneously when $\hat{G}_N^{\text{det}} \in \mathcal{D}_{\text{adm}}(C(\theta_{\text{com}}))$ has been generated by $G_0 \notin \mathcal{D}_{\text{adm}}(C(\theta_{\text{com}}))$. This is in effect a wrong decision since the performance drop is not due to variations

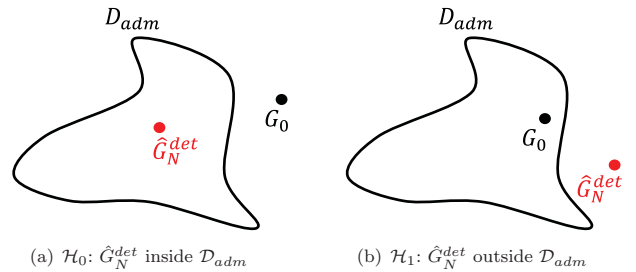


Figure 3. Possibilities of making an erroneous decision in the decision rule (11). (a) \mathcal{H}_0 : \hat{G}_N^{det} inside \mathcal{D}_{adm} . (b) \mathcal{H}_1 : \hat{G}_N^{det} outside \mathcal{D}_{adm} .

in disturbance characteristics, but due to changes in the plant dynamics. Conversely, the choice of the alternative hypothesis \mathcal{H}_1 is erroneous when $G_0 \in \mathcal{D}_{\text{adm}}(C(\theta_{\text{com}}))$.

In hypothesis testing, the accuracy of the decision rule is determined by two probabilities—the probability $Pr_{\mathcal{H}_0}$ of deciding \mathcal{H}_0 when \mathcal{H}_0 is true and the probability $Pr_{\mathcal{H}_1}$ of deciding \mathcal{H}_1 when \mathcal{H}_1 is true

$$Pr_{\mathcal{H}_0} \triangleq Pr\{\hat{G}_N^{\text{det}} \in \mathcal{D}_{\text{adm}}(C(\theta_{\text{com}})) | G_0 \in \mathcal{D}_{\text{adm}}(C(\theta_{\text{com}}))\} \quad (12)$$

$$Pr_{\mathcal{H}_1} \triangleq Pr\{\hat{G}_N^{\text{det}} \notin \mathcal{D}_{\text{adm}}(C(\theta_{\text{com}})) | G_0 \notin \mathcal{D}_{\text{adm}}(C(\theta_{\text{com}}))\}. \quad (13)$$

The probability $Pr_{\mathcal{H}_1}$ is called *detection rate*, whereas the probability $1 - Pr_{\mathcal{H}_0}$ is called *false alarm rate* (Kay, 1998). Clearly, both probabilities $Pr_{\mathcal{H}_0}$ and $Pr_{\mathcal{H}_1}$ should be high for the hypothesis test to be accurate. The probabilities depend not only on the (unknown) true plant dynamics G_0 when the diagnosis experiment is performed³, but also on the accuracy of the identified model \hat{G}_N^{det} . A diagnosis experiment leading to a model \hat{G}_N^{det} very close to G_0 will increase both probabilities. In Section 3, the diagnosis experiment will be designed optimally to guarantee prespecified values for both probabilities $Pr_{\mathcal{H}_0}$ and $Pr_{\mathcal{H}_1}$. Next, the actions that can be performed after performance diagnosis to restore the closed-loop performance are discussed.

2.3 After performance diagnosis

When an observed performance drop is due to variations in disturbance characteristics (\mathcal{H}_0 is the correct hypothesis), it can be decided to let the controller be the same (as disturbance changes are often temporary) or to restore the closed-loop performance by retuning the controller using the knowledge of the new disturbance characteristics \hat{H}_N^{det} identified along with \hat{G}_N^{det} . On the contrary, when an observed performance drop is due to a control-relevant plant change (\mathcal{H}_1 is chosen in (11)), the controller should be re-designed based on a model of the new plant dynamics G_0 to restore the closed-loop performance to its nominal level. As the model $\{\hat{G}_N^{\text{det}}, \hat{H}_N^{\text{det}}\}$ may not be sufficiently accurate for redesigning the controller, the diagnosis step is typically followed by another identification step when \mathcal{H}_1 is the true hypothesis. In this case, a new excitation signal $r_{id}(t)$ is designed and applied to the closed-loop system to collect the data-set $\{u(t), y(t) | t = 0, \dots, N-1\}_{id}$ ⁴.

Since the proposed performance diagnosis approach relies on system identification, a link is established between the diagnosis step and the plant re-identification step. This can be done by identifying the model $\{\hat{G}_N^{id}(z), \hat{H}_N^{id}(z)\}$ not only based on the data $\{u(t), y(t) | t = 0, \dots, N-1\}_{id}$, but also using the data $\{u(t), y(t) | t = 0, \dots, N-1\}_{\text{det}}$ obtained during diagnosis. To this end, a regularisation

term in terms of $\hat{\theta}_N^{\text{det}}$ and its covariance $P_{\hat{\theta}_N^{\text{det}}}$ is defined in (6). The parameter vector of the re-identified plant model $\{\hat{G}_N^{id} = G(z, \hat{\theta}_N^{id}), \hat{H}_N^{id} = H(z, \hat{\theta}_N^{id})\}$ is determined by

$$\hat{\theta}_N^{id} = \arg \min_{\theta} \frac{1}{N} \left(\sum_{t=0}^{N-1} \epsilon^2(t, \theta) + \left\| \theta - \hat{\theta}_N^{\text{det}} \right\|_{P_{\hat{\theta}_N^{\text{det}}}^{-1}}^2 \right),$$

where $\epsilon(t, \theta)$ is computed using $\{u(t), y(t)\}_{id}$. The covariance matrix of $\hat{\theta}_N^{id}$ is given by

$$P_{\hat{\theta}_N^{id}} = \left(\mathcal{I}(\theta_0, \Phi_{r,id}) + \underbrace{\mathcal{I}(\theta_0, \Phi_{r,\text{det}})}_{P_{\hat{\theta}_N^{\text{det}}}^{-1}} \right)^{-1}$$

with $\mathcal{I}(\cdot, \cdot)$ defined as in (10). Using both data-sets to identify $\hat{\theta}_N^{id}$ will enable us to increase the accuracy of $\hat{\theta}_N^{id}$ with respect to the situation where only $\{u(t), y(t) | t = 0, \dots, N-1\}_{id}$ would be used. Note that $P_{\hat{\theta}_N^{\text{det}}}^{-1}$ is an affine function of both $\Phi_{r,id}$ and $\Phi_{r,\text{det}}$ (the spectra of the excitation signals r_{id} and r_{det}). Next, a unified experiment design framework is presented for designing the diagnosis and re-identification experiments where requirements on the diagnosis accuracy are considered along with the requirement on accuracy of the to-be-re-identified model $\hat{G}_N^{id}(z)$.

3. Experiment design framework

This section formulates the optimal experiment design problem for performance diagnosis and possible plant re-identification. The costs associated with performance diagnosis and plant re-identification experiments are first established. The prespecified level of accuracy of the performance diagnosis outcome and the desired accuracy of the to-be-re-identified model (when \mathcal{H}_1 is chosen) are stated in terms of constraints. A so-called two-scenario approach is then presented to obtain initial model estimates that are required for solving the experiment design problem.

3.1 Cost of the diagnosis and re-identification experiments

The objective of the experiment design is to design the spectra $\Phi_{r,\text{det}}$ and $\Phi_{r,id}$ ⁵ of the excitation signals $r_{\text{det}}(t)$ and $r_{id}(t)$. The spectra should be designed such that the total economic cost of performance diagnosis and (possible) plant re-identification is minimised, while guaranteeing the accuracy of performance diagnosis and, if \mathcal{H}_1 is true, the accuracy of the to-be-re-identified model $\hat{G}_N^{id}(z)$. Let us first define the cost of an experiment. Suppose that an experiment of fixed length is performed in the loop $[C(\theta_{\text{com}}) G_0]$ (see Figure 2) using an excitation signal $r(t)$ with spectrum Φ_r . As in Bombois et al. (2006), the experiment cost is

defined as a linear combination of the power of the perturbation signals $y_r(t)$ and $u_r(t)$ induced by the signal $r(t)$ (see (7) and (8))

$$\mathcal{J}(\Phi_r, \theta_0) = \beta_y \left(\frac{1}{2\pi} \int_{-\pi}^{\pi} |G(e^{j\omega}, \theta_0) S_0(e^{j\omega})|^2 \Phi_r(\omega) d\omega \right) + \beta_u \left(\frac{1}{2\pi} \int_{-\pi}^{\pi} |S_0(e^{j\omega})|^2 \Phi_r(\omega) d\omega \right), \quad (14)$$

where β_y and β_u are user specified scalars.

The total economic cost of performance diagnosis and (possible) plant re-identification depends on the outcome of the hypothesis test (11). When \mathcal{H}_0 is true, the cost will only be equal to the cost of the diagnosis experiment ($\mathcal{J}(\Phi_{r,\text{det}}, \theta_0)$). When \mathcal{H}_1 is true, the cost will be equal to the sum of the costs of both diagnosis and re-identification experiments ($\mathcal{J}(\Phi_{r,\text{det}}, \theta_0) + \mathcal{J}(\Phi_{r,\text{id}}, \theta_0)$). However, since the cause of an observed performance drop is not known a priori, the experiment design should be performed considering that both hypotheses can be true. In addition, the experiment cost in both cases of \mathcal{H}_0 and \mathcal{H}_1 depends on the unknown true system parametrised by θ_0 . To address this problem, a so-called two-scenario approach is proposed (see Section 3.3). The two-scenario approach will deliver an a-priori estimate $\theta_{0,\mathcal{H}_0}^{\text{init}}$ of θ_0 for the case when \mathcal{H}_0 is true and an a-priori estimate $\theta_{0,\mathcal{H}_1}^{\text{init}}$ of θ_0 for the case when \mathcal{H}_1 is true. These two estimates can then be used to evaluate the costs of the experiments.

Another important consideration related to the existence of two hypotheses is to determine which cost should be minimised in the optimal experiment design. In this paper, the weighted cost $\mathcal{J}(\Phi_{r,\text{det}}, \theta_{0,\mathcal{H}_1}^{\text{init}}) + \lambda \mathcal{J}(\Phi_{r,\text{id}}, \theta_{0,\mathcal{H}_1}^{\text{init}})$ (corresponding to \mathcal{H}_1) is minimised, while constraining the cost $\mathcal{J}(\Phi_{r,\text{det}}, \theta_{0,\mathcal{H}_0}^{\text{init}})$ (corresponding to \mathcal{H}_0) to be smaller than a user specified threshold β , (i.e., $\mathcal{J}(\Phi_{r,\text{det}}, \theta_{0,\mathcal{H}_0}^{\text{init}}) < \beta$); λ denotes some prespecified weight. The threshold β should be chosen such that it is (much) smaller than the cost of plant re-identification. Next, the quality objectives for the experiment design are described.

3.2 Quality objectives for optimal experiment design

The diagnosis experiment influences the accuracy of the decision rule (11) through affecting the uncertainty of \hat{G}_N^{det} . The model uncertainty can be described by the covariance matrix $P_{\hat{\theta}_N^{\text{det}}}$ (see (9)), which is a function of spectrum Φ_r , det used during the diagnosis experiment. Hence, the accuracy of performance diagnosis can be stated in terms of constraining $Pr_{\mathcal{H}_0}$ and $Pr_{\mathcal{H}_1}$ to be higher than some user specified probabilities α_0 and α_1

$$\begin{aligned} Pr\{\hat{G}_N^{\text{det}} \in \mathcal{D}_{\text{adm}}(C(\theta_{\text{com}})) | G_0 \in \mathcal{D}_{\text{adm}}(C(\theta_{\text{com}}))\} &\geq \alpha_0 \\ Pr\{\hat{G}_N^{\text{det}} \notin \mathcal{D}_{\text{adm}}(C(\theta_{\text{com}})) | G_0 \notin \mathcal{D}_{\text{adm}}(C(\theta_{\text{com}}))\} &\geq \alpha_1. \end{aligned} \quad (15)$$

Due to the dependence of the above constraints on the unknown true plant, the a-priori estimates $\theta_{0,\mathcal{H}_0}^{\text{init}}$ and $\theta_{0,\mathcal{H}_1}^{\text{init}}$ (determined using the two-scenario approach) are required to evaluate (15).

In addition to constraints (15), another constraint is required to guarantee the accuracy of the to-be-re-identified model \hat{G}_N^{id} . The latter constraint is defined in terms of the uncertainty of \hat{G}_N^{id} , which should be small enough to ensure that a controller $C(\hat{\theta}_N^{\text{id}})$ designed with \hat{G}_N^{id} achieves sufficient closed-loop performance ($J(G_0, C(\hat{\theta}_N^{\text{id}}), W_l, W_r) \leq 1$) with the least (user specified) probability level α_{id} . The uncertainty of \hat{G}_N^{id} is described in terms of the covariance matrix $P_{\hat{\theta}_N^{\text{id}}}$, which is a function of Φ_r , det and Φ_r , id. Note that the re-identification constraint depends on the true plant knowledge, which will be approximated by the estimate $\theta_{0,\mathcal{H}_1}^{\text{init}}$ of θ_0 obtained from the two-scenario approach.

3.3 Two-scenario approach

It follows from the previous sections that the optimal experiment design depends on the (unknown) plant dynamics (1). In the event of a performance drop, the model $\{G(z, \theta_{\text{com}}), H(z, \theta_{\text{com}})\}$ obtained at commissioning is no longer (fully) valid. The diagnosis experiment design is further compounded by the fact that it is not known a priori whether the performance drop is due to changes in disturbance characteristics (\mathcal{H}_0 is true) or due to plant changes (\mathcal{H}_1 is true). Hence, the experiment design for performance diagnosis should be performed considering both possible hypotheses. The following hypothetical scenarios are considered to estimate the plant dynamics when \mathcal{H}_0 and \mathcal{H}_1 are true.

- (1) Scenario 1. If \mathcal{H}_0 is true, the performance drop is only due to changes in disturbance characteristics, while the plant dynamics remain the same as that at commissioning. Hence, an adequate model for G_0 is $G(z, \theta_{\text{com}})$, and an estimate for H_0 is identified from routine operating data.
- (2) Scenario 2. If \mathcal{H}_1 is true, the performance drop is only due to changes in the plant dynamics, while the disturbance characteristics are the same as those at commissioning. Hence, an adequate model for H_0 is $H(z, \theta_{\text{com}})$, and an estimate for G_0 is identified from routine operating data.

The above scenarios allow for determining the estimates $\theta_{0,\mathcal{H}_0}^{\text{init}}$ and $\theta_{0,\mathcal{H}_1}^{\text{init}}$ of θ_0 using routine operating data, which correspond to the hypotheses \mathcal{H}_0 and \mathcal{H}_1 , respectively⁶. The model estimates obtained in Scenarios 1 and 2 are denoted by $\{G(z, \theta_{0,\mathcal{H}_0}^{\text{init}}), H(z, \theta_{0,\mathcal{H}_0}^{\text{init}})\}$ and $\{G(z, \theta_{0,\mathcal{H}_1}^{\text{init}}), H(z, \theta_{0,\mathcal{H}_1}^{\text{init}})\}$, respectively. To reformulate the constraints (15) in terms of the estimates $\theta_{0,\mathcal{H}_0}^{\text{init}}$ and $\theta_{0,\mathcal{H}_1}^{\text{init}}$, the following properties of the estimates with respect to $\mathcal{D}_{\text{adm}}(C(\theta_{\text{com}}))$ are used

$$G(z, \theta_{0, \mathcal{H}_0}^{\text{init}}) = G(z, \theta_{\text{com}}) \in \mathcal{D}_{\text{adm}}(C(\theta_{\text{com}})) \quad (16)$$

$$G(z, \theta_{0, \mathcal{H}_1}^{\text{init}}) \notin \mathcal{D}_{\text{adm}}(C(\theta_{\text{com}})). \quad (17)$$

These properties follow directly from the definition of Scenarios 1 and 2. Note that (17) can only be guaranteed asymptotically.

3.4 Formulation of the optimal experiment design problem

The optimal experiment design problem is formulated using the a-priori estimates $\theta_{0, \mathcal{H}_0}^{\text{init}}$ and $\theta_{0, \mathcal{H}_1}^{\text{init}}$ of the true plant, the properties (16) and (17), the definition of $\mathcal{D}_{\text{adm}}(C(\theta_{\text{com}}))$, and the distribution of $\hat{\theta}_N^{\text{det}}$. The experiment design problem is defined as determining the spectra $\Phi_{r, \text{det}}$ and $\Phi_{r, id}$ through minimising the objective function

$$\mathcal{J}(\Phi_{r, \text{det}}, \theta_{0, \mathcal{H}_1}^{\text{init}}) + \lambda \mathcal{J}(\Phi_{r, id}, \theta_{0, \mathcal{H}_1}^{\text{init}}) \quad (18)$$

under the constraints

$$\mathcal{J}(\Phi_{r, \text{det}}, \theta_{0, \mathcal{H}_0}^{\text{init}}) < \beta \quad (19)$$

$$\Pr \left\{ \begin{array}{l} J(G(\hat{\theta}_N^{\text{det}}), C(\theta_{\text{com}}), W_l, W_r) \\ \leq 1 \mid \hat{\theta}_N^{\text{det}} \sim \mathcal{N}(\theta_0 \triangleq \theta_{0, \mathcal{H}_0}^{\text{init}}, P_{\hat{\theta}_N^{\text{det}}}) \end{array} \right\} \geq \alpha_0 \quad (20)$$

$$\Pr \left\{ \begin{array}{l} J(G(\hat{\theta}_N^{\text{det}}), C(\theta_{\text{com}}), W_l, W_r) \\ > 1 \mid \hat{\theta}_N^{\text{det}} \sim \mathcal{N}(\theta_0 \triangleq \theta_{0, \mathcal{H}_1}^{\text{init}}, P_{\hat{\theta}_N^{\text{det}}}) \end{array} \right\} \geq \alpha_1 \quad (21)$$

and a constraint for guaranteeing the accuracy of the to-be-re-identified model, for which $\theta_{0, \mathcal{H}_1}^{\text{init}}$ is used as an estimate of the true plant (see (25)). Note that in (20) and (21), the covariance matrix $P_{\hat{\theta}_N^{\text{det}}}$ will be evaluated in terms of $\mathcal{I}(\theta_{0, \mathcal{H}_0}^{\text{init}}, \Phi_{r, \text{det}})^{-1}$ and $\mathcal{I}(\theta_{0, \mathcal{H}_1}^{\text{init}}, \Phi_{r, \text{det}})^{-1}$, respectively.

To determine the optimal spectrum $\Phi_{r, \text{det}}$, the constraints (20) and (21) are reformulated using a confidence region U that can be constructed based on the normal distribution of $\hat{\theta}_N^{\text{det}}$. Assuming that $\hat{\theta}_N \sim \mathcal{N}(\theta_0, P)$, then $\Pr(\hat{\theta}_N \in U(\theta_0, P^{-1}, \alpha)) = \alpha$, where

$$U(\theta_0, P^{-1}, \alpha) \triangleq \{\theta \mid (\theta - \theta_0)^T P^{-1} (\theta - \theta_0) < \mathcal{X}(\alpha)\} \quad (22)$$

and \mathcal{X} is a real constant such that $\Pr(\chi^2(k) < \mathcal{X}(\alpha)) = \alpha$. $\chi^2(k)$ is a chi-square distributed random variable with k degrees of freedom (i.e., the number of parameters of $G(z, \theta)$).

Following Jansson and Hjalmarsson (2005), sufficient conditions for the constraints (20) and (21) are

$$J(G(\theta), C(\theta_{\text{com}}), W_l, W_r) \leq 1 \quad \forall \theta \in U(\theta_{0, \mathcal{H}_0}^{\text{init}}, \mathcal{I}_0, \alpha_0) \quad (23)$$

$$J(G(\theta), C(\theta_{\text{com}}), W_l, W_r) > 1 \quad \forall \theta \in U(\theta_{0, \mathcal{H}_1}^{\text{init}}, \mathcal{I}_1, \alpha_1), \quad (24)$$

where $\mathcal{I}_0 = \mathcal{I}(\theta_{0, \mathcal{H}_0}^{\text{init}}, \Phi_{r, \text{det}})$ and $\mathcal{I}_1 = \mathcal{I}(\theta_{0, \mathcal{H}_1}^{\text{init}}, \Phi_{r, \text{det}})$. Equations (23) and (24) directly follow from the constraints (20) and (21) when the confidence region U contains $\hat{\theta}_N^{\text{det}}$ with a probability α_0 and α_1 , respectively. Tighter conditions for constraints (20) and (21) can also be obtained (see Katselis, Rojas, Hjalmarsson, & Bengtsson, 2012 for the finite sample case), but the conditions (23) and (24) are used in this paper.

The constraint on the accuracy of $\hat{\theta}_N^{\text{id}}$ is fulfilled if

$$J(G(\theta), C(\theta_{0, \mathcal{H}_1}^{\text{init}}), W_l, W_r) \leq 1 \quad \forall \theta \in U(\theta_{0, \mathcal{H}_1}^{\text{init}}, \mathcal{I}_{id}, \alpha_{id}) \quad (25)$$

with $\mathcal{I}_{id} = \mathcal{I}(\theta_{0, \mathcal{H}_1}^{\text{init}}, \Phi_{r, \text{det}}) + \mathcal{I}(\theta_{0, \mathcal{H}_1}^{\text{init}}, \Phi_{r, id})$. $\theta_{0, \mathcal{H}_1}^{\text{init}}$ is used here as an estimate of the unknown $\hat{\theta}_N^{\text{id}}$ and, therefore, $U(\theta_{0, \mathcal{H}_1}^{\text{init}}, \mathcal{I}_{id}, \alpha_{id})$ contains the true parameter vector θ_0 with a probability α_{id} . Equation (25) ensures that $J(G_0, C(\hat{\theta}_N^{\text{id}}), W_l, W_r) \leq 1$ with a probability of at least α_{id} . Since the disturbance characteristics are assumed to be the same as those at commissioning (see Scenario 2 in Section 3.3), $J(G_0, C(\hat{\theta}_N^{\text{id}}), W_l, W_r) \leq 1$ will guarantee satisfactory closed-loop performance.

3.5 Solution of the experiment design problem

To solve the experiment design problem, the power spectra $\Phi_{r, \text{det}}$ and $\Phi_{r, id}$ are parameterised as

$$\Phi_r(\omega) = R_r(0) + 2 \sum_{i=1}^m R_r(i) \cos(i\omega) \geq 0 \quad \forall \omega, \quad (26)$$

where m is a positive integer⁷. The sequences $R_{r, \text{det}}(i)$ and $R_{r, id}(i)$ ($i = 0 \dots m$) are the decision variables of the experiment design problem. An LMI constraint should be defined in terms of the sequences $R_{r, \text{det}}(i)$ and $R_{r, id}(i)$ to ensure the positivity of $\Phi_{r, \text{det}}$ and $\Phi_{r, id}$ (see Bombois et al., 2006). The objective function (18) is a linear function of $\Phi_{r, \text{det}}$ and $\Phi_{r, id}$ and, consequently, the decision variables $R_{r, \text{det}}(i)$ and $R_{r, id}(i)$ ($i = 0 \dots m$). The same holds for the constraint (19).

Using (3), the constraints (23) and (25) are equivalent to the following frequency-dependent constraints that should hold at each frequency $\omega \in [0 \pi]$

$$\bar{J}(\omega, G(\theta), C(\theta_{\text{com}}), W_l, W_r) \leq 1 \quad \forall \theta \in U(\theta_{0, \mathcal{H}_0}^{\text{init}}, \mathcal{I}_0, \alpha_0) \quad (27)$$

$$\bar{J}(\omega, G(\theta), C(\theta_{0,\mathcal{H}_1}^{\text{init}}), W_l, W_r) \leq 1 \quad \forall \theta \in U(\theta_{0,\mathcal{H}_1}^{\text{init}}, \mathcal{I}_{id}, \alpha_{id}). \quad (28)$$

Note that instead of gridding the frequency axis, the Kalman–Yakubovich–Popov lemma can be used to obtain a frequency independent LMI (Jansson & Hjalmarsson, 2005).

The interval $[0, \pi]$ is discretised to obtain a frequency grid Ω and, consequently, a finite number of constraints. The constraints (27) and (28) can be formulated as LMI constraints in the decision variables $R_{r,\text{det}}(i)$ and $R_{r,\text{id}}(i)$ ($i = 0 \dots m$). This follows from the fact that (27) and (28) can be transformed into LMI constraints in the variables \mathcal{I}_0 and \mathcal{I}_{id} , respectively, and that the covariance matrices are affine functions of $\Phi_{r,\text{det}}$ and $\Phi_{r,\text{id}}$ (Bombois et al., 2006). On the other hand, the constraint (24) is satisfied if for any given frequency ω^*

$$\bar{J}(\omega^*, G(\theta), C(\theta_{\text{com}}), W_l, W_r) > 1 \quad \forall \theta \in U(\theta_{0,\mathcal{H}_1}^{\text{init}}, \mathcal{I}_1, \alpha_1), \quad (29)$$

where the frequency ω^* can be chosen as

$$\omega^* = \arg \max_{\omega} \bar{J}(\omega, G(\theta_{0,\mathcal{H}_1}^{\text{init}}), C(\theta_{\text{com}}), W_l, W_r). \quad (30)$$

The constraint (29) is transformed into an LMI constraint in the variables \mathcal{I}_1 (see Appendix 1) and, consequently, in the decision variables $R_{r,\text{det}}(i)$ ($i = 0 \dots m$).

It follows from above that if $\Phi_{r,\text{det}}$ and $\Phi_{r,\text{id}}$ are parameterised as in (26), the optimal experiment design problem presented in Section 3.4 can be stated as an LMI optimisation problem

$$\begin{aligned} \min_{\Phi_{r,\text{det}}, \Phi_{r,\text{id}}} \quad & \mathcal{J}(\Phi_{r,\text{det}}, \theta_{0,\mathcal{H}_1}^{\text{init}}) + \lambda \mathcal{J}(\Phi_{r,\text{id}}, \theta_{0,\mathcal{H}_1}^{\text{init}}) \\ \text{s.t.} \quad & \mathcal{J}(\Phi_{r,\text{det}}, \theta_{0,\mathcal{H}_0}^{\text{init}}) < \beta \\ & \bar{J}(\omega, G(\theta), C(\theta_{\text{com}}), W_l, W_r) \leq 1, \\ & \quad \forall \theta \in U(\theta_{0,\mathcal{H}_0}^{\text{init}}, \mathcal{I}_0, \alpha_0), \quad \forall \omega \in \Omega \\ & \bar{J}(\omega^*, G(\theta), C(\theta_{\text{com}}), W_l, W_r) > 1, \\ & \quad \forall \theta \in U(\theta_{0,\mathcal{H}_1}^{\text{init}}, \mathcal{I}_1, \alpha_1) \\ & \bar{J}(\omega, G(\theta), C(\theta_{0,\mathcal{H}_1}^{\text{init}}), W_l, W_r) \leq 1, \\ & \quad \forall \theta \in U(\theta_{0,\mathcal{H}_1}^{\text{init}}, \mathcal{I}_{id}, \alpha_{id}), \quad \forall \omega \in \Omega. \end{aligned} \quad (31)$$

Remark 2: Instead of choosing ω^* as in (30), the optimisation problem (31) can be solved for different values of ω^* . The optimal spectra are those corresponding to the frequencies ω^* that result in the smallest objective function.

4. Performance diagnosis and plant re-identification in practice

Before illustrating the experiment design procedure with a simulation case study, this section discusses how the results of the experiment design will be implemented in practice. The outcomes of the experiment design are the optimal spectra $\Phi_{r,\text{det}}$ and $\Phi_{r,\text{id}}$. When the latter spectra are computed, the performance diagnosis experiment is performed by applying the signal r_{det} with spectrum $\Phi_{r,\text{det}}$ to the closed-loop system $[C(\theta_{\text{com}})G_0]$. Based on the collected data, a model \hat{G}_N^{det} of G_0 is identified and, subsequently, it is verified whether \hat{G}_N^{det} lies in $\mathcal{D}_{\text{adm}}(C(\theta_{\text{com}}))$ (see the decision rule (11)).

If $\hat{G}_N^{\text{det}} \notin \mathcal{D}_{\text{adm}}(C(\theta_{\text{com}}))$, plant re-identification should be performed. An excitation signal with spectrum $\Phi_{r,\text{id}}$ (determined together with $\Phi_{r,\text{det}}$) can be used for plant re-identification. Alternatively, the spectrum $\Phi_{r,\text{id}}$ can be redesigned using $\hat{\theta}_N^{\text{det}}$ as an estimate for the true system (instead of using $\theta_{0,\mathcal{H}_1}^{\text{init}}$). Clearly, the estimate $\hat{\theta}_N^{\text{det}}$ provides a more accurate description of the true system, since it has been identified using an external excitation signal.

Note that the optimal performance diagnosis experiment is designed to guarantee a prespecified diagnosis accuracy ($Pr_{\mathcal{H}_0} > \alpha_0$ and $Pr_{\mathcal{H}_1} > \alpha_1$). Since the choice of \mathcal{H}_1 would necessitate plant re-identification with high accuracy (which typically incur high economic cost), the decision rule (11) can be modified slightly to reduce the false alarm rate (i.e., the probability of choosing \mathcal{H}_1 when \mathcal{H}_0 is true). The modified decision rule then consists in choosing \mathcal{H}_1 only when the following two conditions are met:

- (1) $\hat{G}_N^{\text{det}} \notin \mathcal{D}_{\text{adm}}(C(\theta_{\text{com}}))$
- (2) There does not exist a model G within $\mathcal{D}_{\text{adm}}(C(\theta_{\text{com}}))$ that can explain the data $\{u(t), y(t) \mid t = 0, \dots, N-1\}_{\text{det}}$ with a fit similar to the one of the model $\hat{G}_N^{\text{det}} \notin \mathcal{D}_{\text{adm}}(C(\theta_{\text{com}}))$.

The implementation of the modified decision rule is discussed in Appendix 2.

5. Case study: a continuous stirred tank reactor

The presented performance diagnosis approach is applied to a continuous stirred tank reactor (CSTR), in which the exothermic reaction $A \rightarrow B$ occurs. The process dynamics are described by

$$\begin{aligned} V \frac{dC_A}{dt} &= F(C_{A,\text{in}} - C_A) - VR \\ \rho V C_p \frac{dT}{dt} &= \rho F C_p (T_{\text{in}} - T) + \Delta H V R - UA(T - T_c), \end{aligned} \quad (32)$$

Table 1. Linearised models of the nonlinear process model (32) obtained for the different operating scenarios. Scenario 1 pertains to a change in the variance of the feed composition $\bar{C}_{A,\text{in}}$ (defined in terms of a white-noise process with variance σ_e^2), whereas Scenario 2 pertains to a shift (due to a permanent process disturbance) in the operating point around which (32) is linearized.

Nominal operation:	$\bar{C}_A = \underbrace{\frac{19.52z^{-1} + 4.58z^{-2}}{1 + 0.38z^{-1} + 0.04z^{-2}}}_{G_0} \bar{F} + \underbrace{\frac{33.18z^{-1} + 7.79z^{-2}}{1 + 0.38z^{-1} + 0.04z^{-2}}}_{H_0} \bar{C}_{A,\text{in}}$	$\sigma_e^2 = 1.0$
Scenario 1:	$\bar{C}_A = \underbrace{\frac{19.52z^{-1} + 4.58z^{-2}}{1 + 0.38z^{-1} + 0.04z^{-2}}}_{G_0} \bar{F} + \underbrace{\frac{33.18z^{-1} + 7.79z^{-2}}{1 + 0.38z^{-1} + 0.04z^{-2}}}_{H_0} \bar{C}_{A,\text{in}}$	$\sigma_e^2 = 5.0$
Scenario 2:	$\bar{C}_A = \underbrace{\frac{19.52z^{-1} + 3.89z^{-2}}{1 + 1.1z^{-1} + 0.99z^{-2}}}_{G_0} \bar{F} + \underbrace{\frac{33.18z^{-1} + 6.44z^{-2}}{1 + 1.1z^{-1} + 0.99z^{-2}}}_{H_0} \bar{C}_{A,\text{in}}$	$\sigma_e^2 = 1.0$

where the reactant concentration C_A (kg/m³) and the reactor temperature T (K) comprise the system states; V denotes the reactor volume (m³); F denotes the feed flow rate (m³/s); $C_{A,\text{in}}$ denotes the reactant concentration in the feed (kg/m³); ρ and C_p denote the density (kg/m³) and the specific heat capacity (J/kgK) of the reaction medium; ΔH denotes the heat of reaction (J/kg); UA denotes the overall heat transfer coefficient (J/sK); T_c denotes the temperature of the cooling medium (K); and R denotes the reaction rate defined by

$$R = k_0 e^{-\frac{E_a}{RT}} C_A^2$$

with k_0 , E_a , and R being the reaction rate constant (m³/kgs), the activation energy (J/mol), and the universal gas constant (J/mol K), respectively (see Russo & Bequette, 1997 for a detailed description of the process model).

The process model (32) has been linearised around its steady state in order to describe the dynamics of the measured process output C_A in response to variations in the process input F (feed flow rate) and the process disturbance $C_{A,\text{in}}$ (feed composition) around the nominal operating point. The plant model $G(z, \theta_0)$ and the disturbance model $H(z, \theta_0)$ obtained for the (desired) nominal operating point are given in Table 1 in terms of the deviation variables \bar{C}_A , \bar{F} , and $\bar{C}_{A,\text{in}}$. Assuming that the knowledge of the true plant is available, the nominal plant model in Table 1 has been used to design an H_∞ -controller $C(\theta_{\text{com}})$. The performance weight filters in (2) have been selected as

$$W_l = \text{diag} \left(0, \frac{0.52z^{-1} - 0.46z^{-2}}{1.2 - 0.99z^{-1} + 0.51z^{-2}} \right) \quad \text{and} \\ W_r = \text{diag}(0, 1),$$

which allow for defining the measure J uniquely in terms of the sensitivity function (relating $v(t) = H_0(z)e(t)$ and $y(t)$).

The weight W_{l2} has been chosen such that

$$\left| \frac{1}{1 + C(e^{j\omega}, \theta_{\text{com}})G_0(e^{j\omega})} \right| < |W_{l2}(e^{j\omega})|^{-1},$$

which implies that $J(G_0, C(\theta_{\text{com}}), W_l, W_r) \leq 1$ or, equivalently, $G_0 \in \mathcal{D}_{\text{adm}}(C(\theta_{\text{com}}))$ at commissioning. The performance of the closed-loop system is assessed in terms of the variance of the output signal. The controller $C(\theta_{\text{com}})$ has been designed such that it leads to a sufficiently small variance of the output signal at commissioning. At the commissioning stage of the controller, the variance of the process output is $\sigma_y^2 = 1.47$.

Next, two cases that pertain to two different operation scenarios of the CSTR are considered to demonstrate the presented experiment design approach for performance diagnosis.

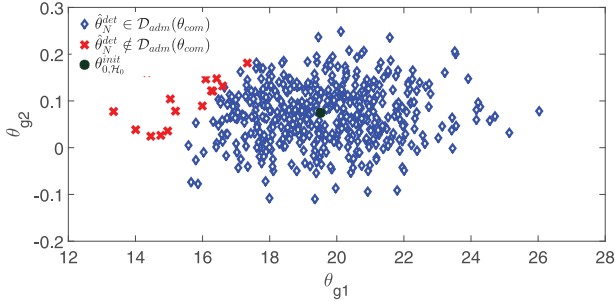
Scenario 1 (changes in characteristics of the feed composition $C_{A,\text{in}}$).

Scenario 1 corresponds to a change in the variance of the feed composition $C_{A,\text{in}}$, which has undergone a five-fold increase (see Table 1 for the process model under this operation scenario). In real practice, such changes in the feed composition of the reactor often arise from variations in the upstream units of the reactor, and can be regarded as temporary disturbances. The change in characteristics of the disturbance $C_{A,\text{in}}$ leads to a significant increase in the variance of the process output ($\sigma_y^2 = 4.27$), suggesting that the closed-loop performance has deteriorated. Note that since the plant is the same as that under the nominal operation scenario, G_0 still lies in $\mathcal{D}_{\text{adm}}(C(\theta_{\text{com}}))$. Therefore, hypothesis \mathcal{H}_0 is the correct hypothesis.

To perform the optimal experiment design procedure, the two-scenario approach presented in Section 3.3 is used to obtain the initial estimates $\theta_{0,\mathcal{H}_0}^{\text{init}}$ and $\theta_{0,\mathcal{H}_1}^{\text{init}}$ through collecting 1000 samples of $\{u(t), y(t)\}$ during the routine closed-loop operation. The latter plant estimates are used to solve the experiment design problem (31) with the settings listed in Table 2⁸. The designed optimal spectrum $\Phi_{r,\text{det}}$ is used

Table 2. Settings of the experiment design problem.

	Scenario 1	Scenario 2
N	500	500
β	0.1	0.1
α_0	95.0%	50.0%
α_1	80.0%	95.0%
α_{id}	99.8%	99.8%

Figure 4. Depiction of the identified parameters in Scenario 1 (i.e., $G_0 \in \mathcal{D}_{adm}$) when the designed detection signal is applied to excite the closed-loop system under 500 different noise realisations.

to generate a signal r_{det} of length $N = 500$ for the performance diagnosis experiment⁹. The signal r_{det} is applied to the closed-loop system made up of the controller $C(\theta_{com})$ and the true plant (given in Table 1) to collect data for the identification of $G(\hat{\theta}_N^{det})$. The diagnosis experiment is repeated 500 times with different noise realisations. The results of the Monte Carlo simulation are shown in Figure 4, where θ_{g1} and θ_{g2} denote two of the parameters of the identified plant models $G(\hat{\theta}_N^{det})$. The simulation results suggest that approximately 97% of the identified models $G(\hat{\theta}_N^{det})$ lie in the set $\mathcal{D}_{adm}(C(\theta_{com}))$ and, therefore, the decision rule (11) will lead to the correct decision \mathcal{H}_0 in 97% of the cases. Hence, the constraint $Pr_{\mathcal{H}_0} > \alpha_0$ is fulfilled.

Table 3 lists the excitation costs $\mathcal{J}(\Phi_{r,det}, \theta_0)$ associated with the optimal excitation spectrum $\Phi_{r,det}$. The excitation cost for detection will be approximately 11% lower when the closed-loop system is excited with the designed signal r_{det} as compared to excitation with an input signal with flat spectrum ($m = 0$). Note that in this scenario, re-

Table 3. Excitation costs (for detection and plant re-identification) associated with the optimal excitation signals and signals with flat spectrum.

	Scenario 1		Scenario 2	
	Flat spectrum	Flexible spectrum	Flat spectrum	Flexible spectrum
$\mathcal{J}(\Phi_{r,det}, \theta_0)$	0.097	0.897	0.0017	0.0014
$\mathcal{J}(\Phi_{r,id}, \theta_0)$	NA	NA	0.0014	0.0012

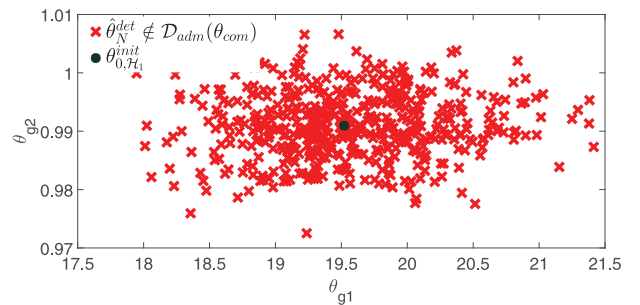
identification of the plant dynamics for redesigning the controller will not be performed, as the observed closed-loop performance drop has originated from (temporary) process disturbances.

Scenario 2 (changes in the plant dynamics due to a shift in the operating point).

Scenario 2 corresponds to a shift in the operating point of the reactor, which has arisen from an upset (permanent process disturbance) in the temperature of the cooling medium regulating the reactor temperature. The nonlinear process model (32) has been linearised around the new operating point to obtain the linear plant model given in Table 1. The closed-loop operation of the controller $C(\theta_{com})$ (developed at the commissioning) with the new plant leads to higher variance of the process output ($\sigma_y^2 = 2.37$), which indicates that the closed-loop performance has degraded with respect to the nominal operating conditions. In Scenario 2, $\mathcal{J}(G_0, C(\theta_{com}), W_l, W_r) > 1$ and, therefore, $G_0 \notin \mathcal{D}_{adm}(C(\theta_{com}))$. Hence, \mathcal{H}_1 is the correct hypothesis in the decision rule (11).

Similar to Scenario 1, the two-scenario approach is used to obtain the initial estimates $\theta_{0,\mathcal{H}_0}^{init}$ and $\theta_{0,\mathcal{H}_1}^{init}$ for solving the experiment design problem (31) with the settings listed in Table 2. The optimal power spectrum $\Phi_{r,det}$ is used to generate a signal r_{det} for the diagnosis experiment. The signal r_{det} is applied to the loop made up of the controller $C(\theta_{com})$ and the true plant to collect data for identification of $G(\hat{\theta}_N^{det})$. The diagnosis experiment has been repeated 500 times with different noise realisations. As shown in Figure 5, the results of the Monte Carlo simulation indicate that 100% of the identified models $G(\hat{\theta}_N^{det})$ lie outside the set $\mathcal{D}_{adm}(C(\theta_{com}))$ and, therefore, the constraint $Pr_{\mathcal{H}_1} > \alpha_1$ is satisfied.

Since \mathcal{H}_1 is chosen in the decision rule (11), a re-identification experiment should follow the diagnosis experiment. This is to obtain a model $G(\hat{\theta}_N^{id})$ of the true plant to design a new controller $C(\hat{\theta}_N^{id})$ for restoration of the degraded closed-loop performance. Thus, the spectrum $\Phi_{r,id}$ determined together with $\Phi_{r,det}$ by the optimal experiment

Figure 5. Depiction of the identified parameters in Scenario 2 (i.e., $G_0 \notin \mathcal{D}_{adm}$) when the designed detection signal is applied to excite the closed-loop system under 500 different noise realisations.

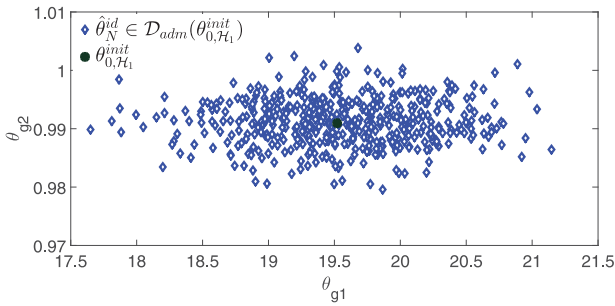


Figure 6. Depiction of the identified parameters of model \hat{G}_N^{id} in Scenario 2 (under 500 different noise realizations) obtained using the designed re-identification signal. The identified model \hat{G}_N^{id} is used to design a new controller $C(\hat{\theta}_N^{id})$ that restores the closed-loop performance.

design problem (31) is used to excite the closed-loop system. The re-identification signal r_{id} with the optimal power spectrum $\Phi_{r,id}$ is applied to the closed-loop system to collect data of length $N = 500$ for plant re-identification. The re-identified model is then used to redesign the controller based on the weight filters given above. The re-identification experiment (and the subsequent controller redesign) is repeated 500 times under different noise realisations. The results of the Monte Carlo simulation suggest that 100% of the redesigned controllers ensure satisfactory closed-loop performance ($J(G_0, C(\hat{\theta}_N^{id}), W_l, W_r) \leq 1$), which is higher than the prespecified probability $\alpha_{id} = 99.8\%$ (see Figure 6). Table 3 indicates that the overall excitation cost $\mathcal{J}(\Phi_{r,det}, \theta_0) + \mathcal{J}(\Phi_{r,id}, \theta_0)$ with the designed signals is smaller than the case in which the diagnosis and re-identification experiment designs are performed independently using signals with a flat spectrum ($m = 0$). The unified experiment design framework reduces the overall excitation cost by approximately 13%.

6. Conclusions

A methodology is developed to address the problem of the closed-loop performance diagnosis. The proposed methodology uses the closed-loop system identification to detect whether an observed performance drop is due to changes in the plant dynamics or due to variations in disturbance characteristics. An experiment design framework is presented for optimal design of the excitation signal used for performance diagnosis, taking into account that a re-identification experiment can follow the diagnosis experiment. The experiment design framework minimises the overall excitation cost incurred for performance diagnosis and plant re-identification, while achieving a desired diagnosis accuracy and a predetermined accuracy for the to-be-re-identified model. The application of the presented framework to a CSTR demonstrates the capability of the performance diagnosis approach in detecting the cause of an observed closed-loop performance drop under fairly realistic (non-linear) process settings.

Disclosure statement

No potential conflict of interest was reported by the authors.

Funding

The research leading to this paper has received funding from the European Union's Seventh Framework Programme (FP7/2007-2013) [grant agreement 257059] (The Autoprofit project, www.fp7-autoprofit.eu).

Notes

1. This work does not consider sensor and actuator failures, even though such failures can in principle be accounted for in the plant dynamics. E.g., self-validating sensors and actuators (Henry & Clarke, 1993; Yang & Clarke, 1999) can be used for dealing with sensor and actuator failures.
2. The closed-loop performance diagnosis approach is extended to model predictive control systems in Bombois, Potters, and Mesbah (2014).
3. In other words, $Pr_{\mathcal{H}_0}$ and $Pr_{\mathcal{H}_1}$ will be different for different plant changes.
4. For notational simplicity, it is assumed that the measurement sets $\{u(t), y(t)\}_{det}$ and $\{u(t), y(t)\}_{id}$ have the same length N .
5. The length of the experiments is supposed fixed a priori.
6. When the routine operating data is not sufficiently informative (i.e., when the data leads to estimates with a large variance), a white-noise signal can be used to excite the plant to collect input/output data for the two-scenario approach (e.g., see Gevers, Bazanella, Bombois, & Miskovic, 2009).
7. The parameters $R_r(i)$ in (26) can be considered as the autocorrelation sequence of a signal that has been generated by passing a white-noise signal through an finite impulse response (FIR) filter of length $m + 1$.
8. The experiment design settings in Table 2 are user specified and are largely dependent on the dynamical characteristics of the system under investigation. Clearly, larger values for probabilities α_0 , α_1 , and α_{id} will lead to more accurate performance diagnosis and plant re-identification results. However, this will be achieved at the expense of a higher experimentation cost β , which should be chosen sufficiently large to ensure the feasibility of the experiment design problem.
9. Note that the optimal $\Phi_{r,id}$ will not be used in Scenario 1.
10. The frequency ω^* can be chosen as $\omega^* = \arg \max_{\omega} \bar{J}(\omega, G(\hat{\theta}_N^{det}), C(\theta_{com}), W_l, W_r)$.

References

- Benveniste, A., Basseville, M., & Moustakides, G.V. (1987). The asymptotic local approach to change detection and model validation. *IEEE Transactions on Automatic Control*, *AC-32*, 583–592.
- Basseville, M. (1998). On-board component fault detection and isolation using the statistical local approach. *Automatica*, *34*, 1391–1415.
- Basseville, M., & Benveniste, A. (1983). Sequential segmentation of nonstationary digital signals using spectral analysis. *Information Sciences*, *29*, 57–73.
- Bombois, X., Gevers, M., Scorletti, G., & Anderson, B.D.O. (2001). Robustness analysis tools for an uncertainty set obtained by prediction error identification. *Automatica*, *37*, 1629–1636.

Bombois, X., Potters, M., & Mesbah, A. (2014). Closed-loop performance diagnosis for model predictive control systems. In *Proceedings of the European Control Conference* (pp. 264–269). Strasbourg: IEEE.

Bombois, X., Scorletti, G., Gevers, M., Van den Hof, P.M.J., & Hildebrand, R. (2006). Least costly identification experiment for control. *Automatica*, 42, 1651–1662.

Gevers, M., Bazanella, A.S., Bombois, X., & Miskovic, L. (2009). Identification and the information matrix: How to get just sufficiently rich? *IEEE Transactions on Automatic Control*, 54, 2828–2840.

Gustafsson, F., & Graebe, S.F. (1998). Closed-loop performance monitoring in the presence of system changes and disturbances. *Automatica*, 34, 1311–1326.

Henry, M.P., & Clarke, D.W. (1993). The self-validating sensor: Rational, definitions and examples. *Control Engineering Practice*, 1, 585–610.

Hjalmarsson, H. (2009). System identification of complex and structured systems. *European Journal of Control*, 15, 275–310.

Huang, B., & Shah, S. (1999). *Performance assessment of control loops. Theory and applications*. London: Springer-Verlag.

Huang, B., & Tamayo, E.C. (2000). Model validation for industrial model predictive control systems. *Chemical Engineering Science*, 55, 2315–2327.

Jansson, H., & Hjalmarsson, H. (2005). Input design via LMIs admitting frequency-wise model specifications in confidence regions. *IEEE Transactions on Automatic Control*, 50(10), 1534–1549.

Jiang, H., Huang, B., & Shah, S.L. (2009). Closed-loop model validation based on the two-model divergence method. *Journal of Process Control*, 19, 644–655.

Katselis, D., Rojas, C.R., Hjalmarsson, H., & Bengtsson, M. (2012). A Chernoff relaxation on the problem of application-oriented finite sample experiment design. In *Proceedings 50th IEEE Conference on Decision and Control* (pp. 202–207). Maui, HI: IEEE.

Kay, S.M. (1998). *Fundamentals of statistical signal processing: Detection theory*. Piscataway, NJ: Prentice Hall.

Ljung, L. (1999). *Systems identification: Theory for the user*. Piscataway, NJ: Prentice Hall.

MacGregor, J., & Cinar, A. (2012). Monitoring, fault diagnosis, fault-tolerant control and optimization: Data driven methods. *Computers and Chemical Engineering*, 47, 111–120.

Olaru, S., De Doná, J.A., & Seron, M.M. (2008). Positive invariant sets for fault tolerant multisensor control schemes. In *Proceedings of the 17th IFAC World Congress* (pp. 1224–1229). Seoul.

Qin, S.J. (2012). Survey on data-driven industrial process monitoring and diagnosis. *Annual Reviews in Control*, 36, 220–234.

Russo, L.P., & Bequette, B.W. (1997). State-space versus input/output representations for cascade control of unstable systems. *Industrial Engineering and Chemistry Research*, 36, 2271–2278.

Seron, M.M., & De Doná, J.A. (2010). Actuator fault tolerant multi-controller scheme using set separation based diagnosis. *International Journal of Control*, 83, 2328–2339.

Shardt, Y., Zhao, Y., Qi, F., Lee, K., Yu, X., Huang, B., & Shah, S. (2012). Determining the state of a process control system: Current trends and future challenges. *The Canadian Journal of Chemical Engineering*, 90, 217–245.

Tyler, M.L., & Morari, M. (1996). Performance monitoring of control systems using likelihood methods. *Automatica*, 32, 1145–1162.

Yang, J.C., & Clarke, D.W. (1999). The self-validating actuator. *Control Engineering Practice*, 7, 249–260.

Yin, S., Ding, S.X., Haghani, A., Hao, H., & Zhang, P. (2012). A comparison study of basic data-driven fault diagnosis and process monitoring methods on the benchmark Tennessee Eastman process. *Journal of Process Control*, 22, 1567–1581.

Zames, G. (1981). Feedback and optimal sensitivity: Model reference transformations, multiplicative seminorms, and approximate inverses. *IEEE Transactions on Automatic Control*, 2, 301–320.

Zhou, K., & Doyle, J. (1998). *Essentials of robust control*. Upper Saddle River, NJ: Prentice Hall.

Appendix 1. LMI formulation of constraint (29)

Proposition 1: Consider the performance measure \bar{J} in (3), the constraint

$$\bar{J}(\omega, G(\theta), C, W_l, W_r) > 1, \quad \forall \theta \in U(\theta_0, \mathcal{I}, \alpha) \quad (\text{A1})$$

at a given frequency ω with U being the confidence region (22), a controller $C(z) = X(z)/Y(z)$, and a parametrisation of the plant $G(z, \theta)$ defined by

$$G(z, \theta) = \frac{Z_N(z)\theta}{1 + Z_D(z)\theta} \quad (\text{A2})$$

with the known vectors Z_N and Z_D . The constraint (A1) is equivalent to the existence of $\tau(\omega) > 0$, $\tau(\omega) \in \mathbf{R}$ such that

$$\begin{pmatrix} \text{Re}(a_{11}) & \text{Re}(a_{12}) \\ \text{Re}(a_{12}^*) & \text{Re}(a_{22}) \end{pmatrix} - \tau \begin{pmatrix} R & -R\theta_0 \\ -(R\theta_0)^T & \theta_0^T R\theta_0 - 1 \end{pmatrix} < 0, \quad (\text{A3})$$

where

$$\begin{aligned} a_{11} &= QZ_1^*Z_1 - (Z_N^*W_{l1}^*W_{l1}Z_N + Z_D^*W_{l2}^*W_{l2}Z_D) \\ a_{12} &= QZ_1^*Y - W_{l2}^*W_{l2}Z_D^* \\ a_{22} &= QY^*Y - W_{l2}^*W_{l2} \\ Z_1 &= XZ_N + YZ_D \\ Q &= \frac{1}{X^*W_{r1}^*W_{r1}X + Y^*W_{r2}^*W_{r2}Y} \\ R &= \frac{\mathcal{I}}{\mathcal{X}(\alpha)} \\ W_l(z) &= \text{diag}(W_{l1}, W_{l2}) \text{ and } W_r = \text{diag}(W_{r1}, W_{r2}). \end{aligned} \quad (\text{A4})$$

Inequality (A3) is affine in the matrix R and, consequently, is affine in the matrix \mathcal{I} .

Proof: Using the definition of $G(z, \theta)$ in (A2), the closed-loop transfer matrix $\mathcal{H}(z, \theta) = W_l F(G(z, \theta), C) W_r$ is expressed as

$$\mathcal{H}(z, \theta) = \begin{pmatrix} \frac{W_{l1}Z_N\theta X W_{r1}}{Y + Z_1\theta} & \frac{W_{l1}Z_N\theta Y W_{r2}}{Y + Z_1\theta} \\ \frac{W_{l2}(1 + Z_D\theta)X W_{r1}}{Y + Z_1\theta} & \frac{W_{l2}(1 + Z_D\theta)Y W_{r2}}{Y + Z_1\theta} \end{pmatrix}, \quad (\text{A5})$$

where $Z_1 = XZ_N + YZ_D$. Since \mathcal{H} is a rank one matrix, (A5) can be rewritten as

$$\mathcal{H}(z, \theta) = \begin{pmatrix} \frac{W_{l1}Z_N\theta}{Y + Z_1\theta} \\ \frac{W_{l2}(1 + Z_D\theta)}{Y + Z_1\theta} \end{pmatrix} (XW_{r1} \quad YW_{r2}). \quad (\text{A6})$$

According to (3), $\bar{J}(\omega, G, C, W_l, W_r) > 1$ implies

$$\bar{\sigma}(\mathcal{H}(e^{j\omega}, \theta)) > 1, \quad (\text{A7})$$

which is equivalent to

$$\bar{\lambda}(\mathcal{H}(e^{j\omega}, \theta)^* \mathcal{H}(e^{j\omega}, \theta)) > 1 \quad (\text{A8})$$

with $\bar{\lambda}(A)$ being the largest eigenvalue of A . Owing to the fact that \mathcal{H} is a rank one matrix, (A8) can be written as

$$1 - \begin{pmatrix} \frac{W_{l1}Z_N\theta}{Y + Z_1\theta} \\ \frac{W_{l2}(1 + Z_D\theta)}{Y + Z_1\theta} \end{pmatrix}^* \begin{pmatrix} \frac{W_{l1}Z_N\theta}{Y + Z_1\theta} \\ \frac{W_{l2}(1 + Z_D\theta)}{Y + Z_1\theta} \end{pmatrix} (X^*W_{r1}^*W_{r1}X - Y^*W_{r2}^*W_{r2}Y) < 0, \quad (\text{A9})$$

where $(\cdot)^*$ denotes the conjugate transpose. The remainder of the proof is similar to that given in Bombois, Gevers, Scorletti, and Anderson (2001).

Appendix 2. Modified decision rule

Suppose that the model \hat{G}_N^{det} identified using data of the performance diagnosis experiment lies outside $\mathcal{D}_{\text{adm}}(C(\theta_{\text{com}}))$ ($J(\hat{G}_N^{\text{det}}, C(\theta_{\text{com}}), W_l, W_r) > 1$). In the modified decision rule, the aim is to verify that there does not exist a model $G(z, \theta) \in \mathcal{D}_{\text{adm}}(C(\theta_{\text{com}}))$ that can describe the data $\{u(t), y(t) | t = 0, \dots, N - 1\}_{\text{det}}$ with a fit similar to the one of the model \hat{G}_N^{det} . The identification cost function $V(\theta)$ (see (6)) computed with the data $\{u(t), y(t) | t = 0, \dots, N - 1\}_{\text{det}}$ can be used to verify if all transfer functions $G(z, \theta^*) \in \mathcal{D}_{\text{adm}}(C(\theta_{\text{com}}))$ fulfil

$$V(\theta^*) - V(\hat{\theta}_N^{\text{det}}) \geq \kappa \quad (\text{A10})$$

for some (large) value κ .

The condition (A10) can be verified using a Taylor expansion around θ_0 , where the expected value of $V(\theta)$ for a given θ is approximated by Hjalmarsson (2009)

$$\mathbb{E}V(\theta) \approx \mathbb{E}V(\theta_0) + \frac{1}{N}(\theta - \theta_0)^T P_{\hat{\theta}_N^{\text{det}}}^{-1}(\theta - \theta_0) \quad (\text{A11})$$

with $P_{\hat{\theta}_N^{\text{det}}}$ defined as in (9). Expression (A11) can be approximated further by replacing θ_0 with its estimate $\hat{\theta}_N^{\text{det}}$ and by neglecting the expected value

$$V(\theta) \approx V(\hat{\theta}_N^{\text{det}}) + \frac{1}{N}(\theta - \hat{\theta}_N^{\text{det}})^T P_{\hat{\theta}_N^{\text{det}}}^{-1}(\theta - \hat{\theta}_N^{\text{det}}). \quad (\text{A12})$$

Hence, the condition (A10) holds for all transfer functions $G(z, \theta^*) \in \mathcal{D}_{\text{adm}}(C(\theta_{\text{com}}))$ if

$$\{G(z, \theta) \mid \theta \in U(\hat{\theta}_N^{\text{det}}, P_{\hat{\theta}_N^{\text{det}}}^{-1}, \alpha_\kappa)\} \in \mathcal{C}\mathcal{D}_{\text{adm}}(C(\theta_{\text{com}})) \quad (\text{A13})$$

with $\mathcal{C}\mathcal{D}_{\text{adm}}(C(\theta_{\text{com}}))$ being the complement of $\mathcal{D}_{\text{adm}}(C(\theta_{\text{com}}))$ and U defined as in (22) such that $Pr(\chi^2(k) < N\kappa) = \alpha_\kappa$.

$\hat{\theta}_N^{\text{det}} \sim \mathcal{N}(\theta_0, P_{\hat{\theta}_N^{\text{det}}})$ implies that θ_0 lies in $U(\hat{\theta}_N^{\text{det}}, P_{\hat{\theta}_N^{\text{det}}}^{-1}, \alpha_\kappa)$ with probability α_κ . Therefore, (A13) indicates that there exists a confidence ellipsoid for θ_0 (with a large probability level) that lies entirely outside $\mathcal{D}_{\text{adm}}(C(\theta_{\text{com}}))$. In other words, the likelihood that $G_0 \in \mathcal{D}_{\text{adm}}(C(\theta_{\text{com}}))$ is negligible.

The condition (A13) is equivalent to

$$J(G(\theta), C(\theta_{\text{com}}), W_l, W_r) > 1, \quad \forall \theta \in U(\hat{\theta}_N^{\text{det}}, P_{\hat{\theta}_N^{\text{det}}}^{-1}, \alpha_\kappa), \quad (\text{A14})$$

which is satisfied if at frequency $\omega^*{}^{10}$

$$\bar{J}(\omega^*, G(\theta), C(\theta_{\text{com}}), W_l, W_r) > 1, \quad \forall \theta \in U(\hat{\theta}_N^{\text{det}}, P_{\hat{\theta}_N^{\text{det}}}^{-1}, \alpha_\kappa). \quad (\text{A15})$$

Note the similarity of (A15) to the constraint (29) of the experiment design problem. It follows from Appendix A that (A15) can be verified in terms of a convex feasibility problem. The largest value of κ (or α_κ), for which (A15) holds, can be determined using a set of linear matrix inequalities.